SICE Annual Conference 2007
Sept. 17-20, 2007, Kagawa University, Japan

Multi-Preview Configuration Control for Redundant Manipulator by Future Reachability Evaluation

Tong-xiao Zhang[1], Mamoru Minami[2] and Wei Song[1]

[1]Graduate school of Engineering, University of Fukui, Bunkyo3-9-1, Fukui, Japan
(Tel : +81-776-27-8527; E-mail: {zhangtongxiao,songwei}@rc.his.fukui-u.ac.jp)
[2]Faculty of Engineering, University of Fukui, Bunkyo3-9-1, Fukui, Japan
(Tel : +81-776-27-8527; E-mail: minami@rc.his.fukui-u.ac.jp)

Abstract: This paper proposes a new approach to achieve an on-line control of trajectory tracking and obstacle avoidance for redundant manipulators without prechecking path-planning in whole trajectory tracking. In the trajectory tarcking process, manipulator is required to keep a configuration with maximal avoidance manipulability in real-time. In this paper, we present a new idea: Multi-Preview Control, which uses several future optimal configurations to control current configuration to complete task of trajectory tracking and obstacle avoidance on-line with high avoidance manipulability and reachability. We verify the validity of multi-preview control through simulations of comparing single-preview control with multi-preview control.

Keywords: Redundant manipulator, Reachability, Multi-preview control, 1-step GA.

1. INTRODUCTION

Over the past two decades, redundant manipulators are used for various kinds of tasks, for example, welding, sealing and contact tasks. These kinds of tasks require the manipulator to plan its hand onto a desired trajectory and avoid its intermediate links from obstacles existing near the target object and also the target object itself.

There are many researches on the motion of redundant manipulators discussing how to use the redundancies. The proposed solutions to this problem can be broadly categorized into two classes: Global and Local Methods. Global Methods (see[1],[2]) solve the collision avoidance problem by an entire path planning. In [2], Ahuactzin and Gupta have proposed an approach to find a reachable configuration (a feasible path) corresponding to a desired position and orientation of end-effector from a given initial configuration of the robot. Such a gobal method's computational cost is very expensive, and usually increases exponentially along with the number of manipulator joints. Moreover, it is obvious that the entire path planning is only suited for structured and static environments and is inapplicable to dynamic environments with moving obstacles. Considering these limitations, global method is implemented only as an off-line path planning tool in the high level of the manipulator control hierarchy. On the other hand, to achieve an ability adaptive to dynamic environments, a system must make efforts to be adaptive as much as possible even in a situation of limited information about surroundings. Such methodology is named as Local Method (see [3],[4]), and this adaptivity requires that the system be flexible for the changing conditions and posess real-time measurement ability. Local Method can deal with moving obstacles in an unstructured workspace. However, to perform the tasks on-line, the information of the environment is limited locally and the computation must be very fast. Otherwise, the arm of the redundant manipulator may be trapped in an undesired situation by Local Methods.

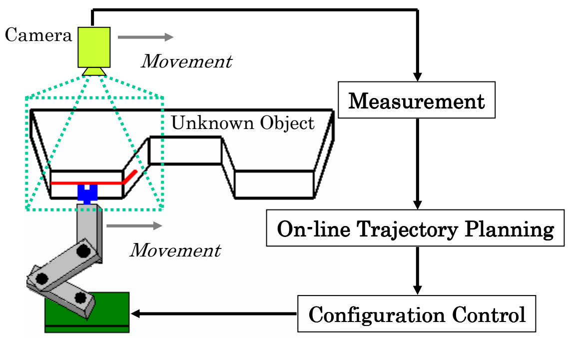

Fig. 1 Processing system for unknown object

Our research also pursues adaptive system in Local Method. However, the most important and meaningful in our system shown in Fig.1 is that it can make the redundant manipulator achieve trajectory tracking and obstacle avoidance smoothly in whole on-line process by using a new on-line control approach: Multi-Preview Control. In Fig.1, the camera and the manipulator's hand are supposed to move in synchrony because achieving on-line operation depends on the real-time information of unknown target object obtained by this moving camera. In reality, the scale of our target object is huge and the area in which the camera can detect the tagret object is relatively small. When the camera detects an obstacle appearing suddenly in the scene, the configuration of manipulator is required to change immediately so that it can avoid this obstacle. Therefore, in the whole on-line trajectory tracking process, always keeping the avoidance manipulability (see[5]) of whole manipulator high is very important. Based on this requirement of high avoidance manipulability, to optimize trajectory tracking and obstacle avoidance on-line, we adopt 1-step Genetic Algorithm (see [6],[7]) considering potential spaces (see [8]) around the measured target object to search real-time optimal

PR0001/07/0000-1011 ¥400 © 2007 SICE

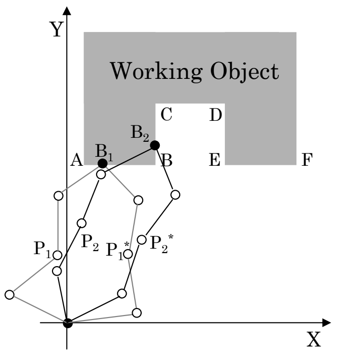

Fig. 2 The concept of single-preview control

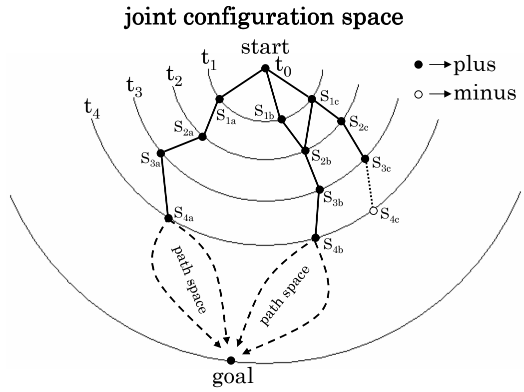

Fig. 3 The concept of multi-preview control

configurations of the manipulator at future times. Then, we present multi-preview control for solving reachability problem according to the concept of preview control (see [9],[10]). These future optimal configurations of imaginary manipulators can control current actual manipulator to achieve on-line trajectory tracking and obstacle avoidance satisfying reachability based on high avoidance manipulability. Comparing the single-preview control used in our previous research with multi-preview control, we exhibit that the limitation of Local Method is reduced in an extent by obtaining more information of trajectory and moving obstacles in the future, which is the most meaningful point of multi-preview control.

2. OVERVIEW OF PREVIEW CONTROL

Our research is to use inverse kinematic knowledge to solve a classical on-line trajectory tracking problem. The position of the manipulator's hand is moving along the trajectory, meanwhile, the joint configuration corresponding to the changing position of the manipulator's hand is also changing for completing trajectory tracking without collision. In addtion, redundancy indicates that one position of the manipulator's hand corresponds to a sub-space in joint configuration space (redundancy solutions). Therefore, trajectory tracking problem in our research includes two main sub-problems: Reachability problem (how to connect in all time all optimal solutions to a goal configuration) and On-line optimization problem (how to select the optimal solution among many solutions in each varying time). In Fig.2, a concept of single-preview control is explained. When the hand reaches the position B_1, two kinds of the manipulator's configurations denoted by P_1 and ${P_1}^*$ both can avoid collision. However, when the hand reaches the position B_2, only the configuration of ${P_2}^*$ in the two configurations denoted by P_2 and ${P_2}^*$ can avoid collision. If the manipulator's configuration is selected as P_1 at hand point B_1, the angular velocities of joints will be high values to change its configuration like ${P_2}^*$ near the corner B. This poses a possibility that the manipulator crashes to corner B when the required high angular velocity is over specified maximum velocity of the joint. Therefore, the manipulator's configuration must be prepared to the configuration ${P_1}^*$ that is similar future configuration ${P_2}^*$. This requires that the current manipulator's configuration should be determined in a consideration of one future possible configuration or be determined by several future possible configurations, which is so-call preview control method (see section 5 for details).

A concept of single-preview control is depicted in Fig.2, which controls the current configuration to ${P_1}^*$ by referring the future optimal configuration ${P_2}^*$ evaluated by future possibility to crash. Our approach is best described as: Multi-preview control. Multi-preview control method is to depend on several future optimal configurations to control current manipulator's configuration to achieve on-line trajectory tracking and obstacle avoidance satisfying reachability evaluated by avoidance manipulability. Fig.3 is to explain the importance of multi-preview control. The times defined by t_0, t_1, t_2, t_3 and t_4 respectively in Fig.3. And "•" indicates local optimal configuration at each future time whose evaluation values are plus and are denoted by S_{1a}, S_{1b}, S_{1c} at $t = t_1$, and S_{2a}, S_{2b}, S_{2c} at $t = t_2$ and so on. When current time $t = t_0$, meaning the manipulator stays at initial configuration, optimal reachable path will be chosen as $S_{1c} \rightarrow S_{2c} \rightarrow S_{3c}$ by estimating $S_{ij}(i = 1, 2, 3; j = a, b, c)$, where the other possible sequences $S_{1a} \rightarrow S_{2a} \rightarrow S_{3a}$, $S_{1b} \rightarrow S_{2b} \rightarrow S_{3b}$ and $S_{1c} \rightarrow S_{2b} \rightarrow S_{3b}$ are second or third optimal sequences and so on. Then the configuration at time $t = t_1$ will be controlled to that of S_{1c}. When the current time $t = t_1$, possible future sequences from S_{1c}, $S_{2b} \rightarrow S_{3b} \rightarrow S_{4b}$ and $S_{2c} \rightarrow S_{3c} \rightarrow S_{4c}$ are evaluated. Shall we provide that the value of S_{4c} has minus value represented by "○" meaning future possible configuration from S_{3c} can not avoide clashing against surroundings or target object. Then the configuration controller needs to choose an optimal sequence as $S_{2b} \rightarrow S_{3b} \rightarrow S_{4b}$. By repeating such evaluation of future configuration sequences and possible route changing, multi-preview control system will avoide dangerous sequences connecting to clashing in the future and can widen out the reachable possibility from current configuration to goal configuration.

3. AVOIDANCE MANIPULABILITY

Representing the vector of position and orientation of each link by $\boldsymbol{r}_i \in R^m (i = 1, 2, \cdots, n)$ where m denotes the dimension of working space, n denotes the number of links of manipulator. Representing the vector of joint angle by $\boldsymbol{q} = [q_1, q_2, \cdots, q_n]^T$. $\boldsymbol{r}_i$ is given by (1) as a function of $\boldsymbol{q}$.

$$\boldsymbol{r}_i = \boldsymbol{f}_i(\boldsymbol{q}), (i = 1, 2, \cdots, n) \tag{1}$$

By differentiating (1) by time t, we can obtain (2).

$$\dot{\boldsymbol{r}}_i = \boldsymbol{J}_i(\boldsymbol{q})\dot{\boldsymbol{q}} \tag{2}$$

In (2), $\boldsymbol{J}_i(\boldsymbol{q}) \in R^{m\times n}$ is Jacobian matrix differentiated $\boldsymbol{r}_i$ by $\boldsymbol{q}$. Here we discuss the case that desired trajectory $\boldsymbol{r}_{nd}$ and desired velocity $\dot{\boldsymbol{r}}_{nd}$ of the manipulator's hand are given as primary task. Then, according to (2) we can obtain $\dot{\boldsymbol{q}}$ realized by $\dot{\boldsymbol{r}}_{nd}$.

$$\dot{\boldsymbol{q}} = \boldsymbol{J}_n^+\dot{\boldsymbol{r}}_{nd} + (\boldsymbol{I}_n - \boldsymbol{J}_n^+\boldsymbol{J}_n)\,{}^1\boldsymbol{l} \tag{3}$$

where $\boldsymbol{J}_n$ is Jacobian matrix differentiated $\boldsymbol{r}_n$ by $\boldsymbol{q}$, $\boldsymbol{J}_n^+$ is pseudo-inverse of $\boldsymbol{J}_n$, and ${}^1\boldsymbol{l}$ is an arbitrary vector satisfying ${}^1\boldsymbol{l} \in R^n$. The first term of right side of (3) is the solution to make $\|\dot{\boldsymbol{q}}\|$ minimize in the space of $\dot{\boldsymbol{q}}$ while realizing $\dot{\boldsymbol{r}}_{nd}$. The second term is joint angle velocity components that can change the manipulator's configuration regardless with the influence of $\dot{\boldsymbol{r}}_{nd}$. When the first avoidance subtask is given to the i-th link, in other words, the first demanded avoidance velocity ${}^1\dot{\boldsymbol{r}}_{di}$ is determined by geometric relation of a manipulator with an obstacle. In this research, we think that it is the frist demanded avoidance velocity obtained from an avoidance control system of higher level. The relation of ${}^1\dot{\boldsymbol{r}}_{di}$ and $\dot{\boldsymbol{r}}_{nd}$ is shown in (4) by substituting (3) into (2).

$${}^1\dot{\boldsymbol{r}}_{di} = \boldsymbol{J}_i\boldsymbol{J}_n^+\dot{\boldsymbol{r}}_{nd} + \boldsymbol{J}_i(\boldsymbol{I}_n - \boldsymbol{J}_n^+\boldsymbol{J}_n)\,{}^1\boldsymbol{l} \tag{4}$$

Left side superscript "1" means the first avoidance subtask, i.e., ${}^1\dot{\boldsymbol{r}}_{di}$ denotes that the i-th link is ordered to finish the first avoidance subtask, it is defined as the same meaning in the following explanation. Here we define two variables shown in (5) and (6).

$$\Delta^1\dot{\boldsymbol{r}}_{di} \stackrel{\triangle}{=} {}^1\dot{\boldsymbol{r}}_{di} - \boldsymbol{J}_i\boldsymbol{J}_n^+\dot{\boldsymbol{r}}_{nd} \tag{5}$$

$${}^1\boldsymbol{M}_i \stackrel{\triangle}{=} \boldsymbol{J}_i(\boldsymbol{I}_n - \boldsymbol{J}_n^+\boldsymbol{J}_n) \tag{6}$$

In (5) and (6), $\Delta^1\dot{\boldsymbol{r}}_{di}$ is represented by the first avoidance velocity and ${}^1\boldsymbol{M}_i$ is a $R^{m\times n}$ matrix represented by the first avoidance matrix. According to (5) and (6), $\Delta^1\dot{\boldsymbol{r}}_{di}$ can be rewritten by (7).

$$\Delta^1\dot{\boldsymbol{r}}_{di} = {}^1\boldsymbol{M}_i\,{}^1\boldsymbol{l} \tag{7}$$

The relation between ${}^1\dot{\boldsymbol{r}}_{di}$ and $\Delta^1\dot{\boldsymbol{r}}_{di}$ is shown in Fig.4.

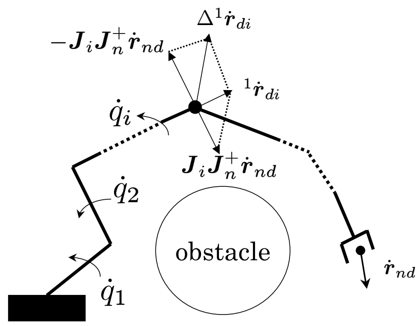

Fig. 4 Obstacle avoidance of intermediate links

Next, we will represent two concepts of avoidance munipulability. One is complete avoidance munipulability ellipsoid, the other is partial avoidance munipulability ellipsoid. When hand velocity $\dot{\boldsymbol{r}}_{nd}$ is given, we can confirm $\boldsymbol{J}_i\boldsymbol{J}_n^+\dot{\boldsymbol{r}}_{nd}$ because $\boldsymbol{J}_i$ and $\boldsymbol{J}_n^+$ have been known. Then, the first demanded avoidance velocity ${}^1\dot{\boldsymbol{r}}_{di}$ is given also. According to (5), we can obtain the first avoidance velocity $\Delta^1\dot{\boldsymbol{r}}_{di}$. However, the problem to be solved is whether we can realize $\Delta^1\dot{\boldsymbol{r}}_{di}$, that is whether we can find ${}^1\boldsymbol{l}$ to realize $\Delta^1\dot{\boldsymbol{r}}_{di}$ because ${}^1\boldsymbol{M}_i$ has been known. From (7), we can obtain ${}^1\boldsymbol{l}$ shown in (8).

$${}^1\boldsymbol{l} = {}^1\boldsymbol{M}_i{}^+\Delta^1\dot{\boldsymbol{r}}_{di} + (\boldsymbol{I}_n - {}^1\boldsymbol{M}_i^+\,{}^1\boldsymbol{M}_i)\,{}^2\boldsymbol{l} \tag{8}$$

In (8), ${}^1\boldsymbol{M}_i^+$ is pseudo-inverse of ${}^1\boldsymbol{M}_i$ and ${}^2\boldsymbol{l}$ is an arbitrary vector satisfying ${}^2\boldsymbol{l} \in R^n$. From (8), we can obtain (9).

$$\|{}^1\boldsymbol{l}\|^2 \geq \Delta^1\dot{\boldsymbol{r}}_{di}{}^T({}^1\boldsymbol{M}_i^+)^T\,{}^1\boldsymbol{M}_i^+\Delta^1\dot{\boldsymbol{r}}_{di} \tag{9}$$

Providing that ${}^1\boldsymbol{l}$ is restricted as $\|{}^1\boldsymbol{l}\| \leq 1$, then the extent where $\Delta^1\dot{\boldsymbol{r}}_{di}$ can move is denoted by (10).

$$\Delta^1\dot{\boldsymbol{r}}_{di}{}^T({}^1\boldsymbol{M}_i^+)^T\,{}^1\boldsymbol{M}_i^+\Delta^1\dot{\boldsymbol{r}}_{di} \leq 1 \tag{10}$$

When $rank({}^1\boldsymbol{M}_i) = m$, $\Delta^1\dot{\boldsymbol{r}}_{di}$ satisfies (11).

$$\Delta^1\dot{\boldsymbol{r}}_{di} = {}^1\boldsymbol{M}_i\,{}^1\boldsymbol{M}_i^+\Delta^1\dot{\boldsymbol{r}}_{di}. \tag{11}$$

In this case, equation (10) represents that the first avoidance velocity $\Delta^1\dot{\boldsymbol{r}}_{di}$ can be described by an ellipsoid expanded in m-dimension space, which indicates $\Delta^1\dot{\boldsymbol{r}}_{di}$ can be freely realized in m-dimension space. The ellipsoid represented by (10) is named as the first complete avoidance manipulability ellipsoid denoted by ${}^{1C}P_i$.

However, when $rank({}^1\boldsymbol{M}_i) = p < m$, a new first avoidance velocity $\Delta^1\dot{\boldsymbol{r}}_{di}^*$ satisfies (12).

$$\Delta^1\dot{\boldsymbol{r}}_{di}^*{}^T({}^1\boldsymbol{M}_i^+)^T\,{}^1\boldsymbol{M}_i^+\Delta^1\dot{\boldsymbol{r}}_{di}^* \leq 1 \tag{12}$$

This new first avoidance velocity $\Delta^1\dot{\boldsymbol{r}}_{di}^*$ can be described by an ellipsoid expanded in p-dimension. The ellipsoid represented by (12) is named as the first partial avoidance manipulability ellipsoid denoted by ${}^{1P}P_i$. Because $p < m$, the first partial avoidance manipulability ellipsoid can be thought as a segment of the first complete avoidance manipulability ellipsoid. Taking a 4-link redundant manipulator in 2-dimension space for example, while the hand of manipulator executes a trajectory tracking task, avoidance manipulability ellipsoids of intermediate links are shown in Fig.5.

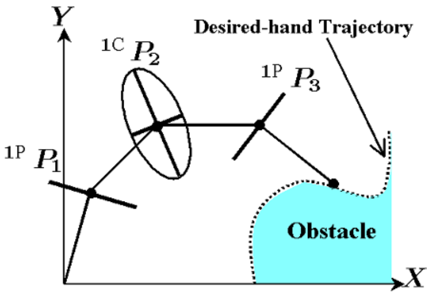

Fig. 5 Avoidance manipulability ellipsoids

According to above discussion, when the hand velocity of manipulator $\dot{\boldsymbol{r}}_{nd}$ is given, it depends on the first avoidance matrix ${}^1\boldsymbol{M}_i$ whether it can realize $\forall\ {}^1\dot{\boldsymbol{r}}_{di} \in R^m$ through the first avoidance velocity $\Delta^1\dot{\boldsymbol{r}}_{di}$.

4. OBSTACLE AVOIDANCE STRATEGY

4.1 AMSI

Here, avoidance manipulability shape index (AMSI) expressed by avoidance manipulability ellipsoid is defined. The volume of avoidance manipulability ellipsoid of i-th link is given as (13).

$$ {}^1V_i = c_m \cdot {}^1w_i \tag{13} $$

where, c_m and ${}^1w_i$ are defined by (14)and (15) respectively.

$$ c_m = \begin{cases} \frac{2(2\pi)^{(m-1)/2}}{1\cdot 3\cdots(m-2)m} & (m : odd) \\ \frac{(2\pi)^{m/2}}{2\cdot 4\cdots(m-2)m} & (m : even) \end{cases} \tag{14} $$

$$ {}^1w_i = {}^1\sigma_{i1}\ {}^1\sigma_{i2} \cdots\ {}^1\sigma_{im} \tag{15} $$

In (15), ${}^1\sigma_{i1},\ {}^1\sigma_{i2}, \cdots,\ {}^1\sigma_{im}$ are the singular values of ${}^1\boldsymbol{M}_i$. When the value of ${}^1V_i$ is the highest, the avoidance manipulability of i-th link is the best.

In this paper, the workspace is assumed by two-dimension to make it comprehensive ($m = 2$). The avoidance manipulability ellipsoid of link2 is the complete avoidance manipulability ellipsoid because $rank({}^1\boldsymbol{M}_2) = 2 = m$. The two singular values of ${}^1\boldsymbol{M}_2$ can denote the length of two axes of ellipsoid. The avoidance manipulability ellipsoids of link1 and link3 are the partial avoidance manipulability ellipsoids because $rank({}^1\boldsymbol{M}_1) = 1 < m$ and $rank({}^1\boldsymbol{M}_3) = 1 < m$, which are expressed by straight lines. Then, AMSI (Avoidance Manipulability Shape Index) denoting avoidance manipulability of whole manipulator is defined by (16).

$$ {}^1E = \sum_{i=1}^{n-1} {}^1V_i a_i \tag{16} $$

where,

$$ a_1 = a_{n-1} = 1[m^{-1}],\ a_{2,3,\cdots,(n-2)} = 1[m^{-2}] \tag{17} $$

When $m = 2$, ${}^1V_1$, ${}^1V_{n-1}$ denote the length, ${}^1V_{2,3,\cdots,(n-2)}$ denote area. By (17), ${}^1E$ denotes a number without unit.

4.2 AMSIP

By using AMSI, although avoidance ability of whole manipulator is the highest, the manipulator will possibly collide with the obstacle because it does not consider the distance between the manipulator and the obstacle. Therefore, we construct the potential spaces along the object's shape detected by camera. This improved index considering collision by constructing the potential spaces is AMSIP. The definition of AMSIP is shown in (18).

$$ {}^1S = {}^1E + U \tag{18} $$

where, $U < 0$ denotes total potential value. Therefore, ${}^1S$ will come down by U and the possibility of the collision will increase once the manipulator moves into potential spaces (detail explanation of potential spaces is shown in [8]).

4.3 Analyses of AMSI and AMSIP

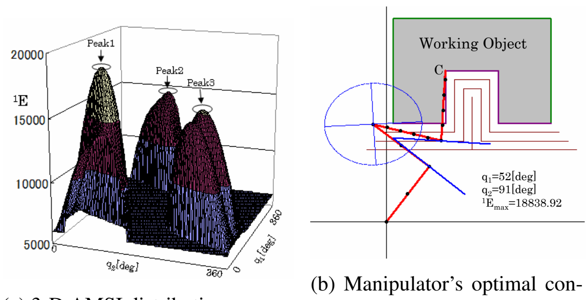

(a) 3-D AMSI distribution

(b) Manipulator's optimal configuration based on AMSI

Fig. 6 3-D AMSI distribution and manipulator's optimal configuration based on AMSI when the hand is fixed at C

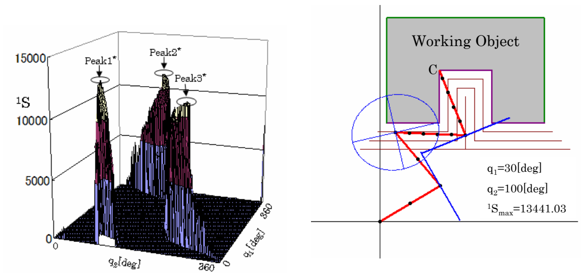

(a) 3-D AMSIP distribution

(b) Manipulator's optimal configuration based on AMSIP

Fig. 7 3-D AMSIP distribution and manipulator's optimal configuration based on AMSIP when the hand is fixed at C

When the manipulator's hand moves to position C in Fig.6(b), the distribution of AMSI about q_1 and q_2 is shown in Fig.6(a), and the distribution of AMSIP is shown in Fig.7(a), where q_1 and q_2 are joint angles of link1 and link2 respectively and they constitute redundancy space of joint angles, q_3 and q_4 are determined depending on the hand position once q_1 and q_2 are confirmed. Comparing Fig.6(a) with Fig.7(a), the obvious difference can be found that the shapes of $Peak^*$ of ${}^1S$ are smaller and thiner than the shapes of $Peak$ of ${}^1E$, moreover there are lots of area corresponding to ${}^1S < 0$ in AMSIP distribution. This fact just indicates that AMSIP depending on the area of ${}^1S < 0$ can avoid the collision successfully. According to Fig.6(b) and Fig.7(b), which denote the manipulator's optimal configurations corresponding to $Peak1$ and $Peak1^*$ respectively, we can find that AMSIP can avoid collision with higher avoidance manipulability. Therefore, we verify that AMSIP is more effective than AMSI.

5. MULTI-PREVIEW CONTROL

5.1 Reachability

Before we present multi-preview control, it is necessary to analyse the concept of reachability. In previous research, we did not concern a key question, that is, whether the current configuration is reachable to the future optimal configuration. Indeed due to moving obstacles in the environment, there may exist an optimal configuration in future time, but there may not be reachable from the current configuration. We assume that the whole tracking process will be finished within 50[s]. We can detect the 3-D AMSIP ${}^1S$ distributions at ten different given times in whole tracking process shown in Fig.8. From Fig.8, we can clearly find that there are four peaks of ${}^1S$ when $t = 0[s]$, $t = 5[s]$ and $t = 10[s]$ denoted by $peak1^*$, $peak2^*$, $peak3^*$ and $peak4^*$ respectively. However, $peak4^*$ disappears from $t = 15[s]$ to end, which indicates the optimal configuration around $peak4^*$ will become dangerous configuration after $15s$ when manipulator's hand tracks the trajectory. In addition, according to Table 1 generalizing the peak values of ${}^1S$, we can think that always keeping ${}^1S$ corresponding to manipulator's configuration around $peak1^*$ in whole tracking process is desired selection, which can satisfy requirement of reachability meanwhile can keep high avoidance ability because $peak1^*$ is always exist and ${}^1S$ around $peak1^*$ is larger than ${}^1S$ of other peaks such as $peak2^*$, $peak3^*$ and $peak4^*$ in whole tracking process.

5.2 Preview Control System

Preview control system depicted in Fig.9 consists of a real-time measurement block, a path planning block, a redundancy control block and a redundant manipulator. On the assumption that current time is represented by t, and the future time is defined as $t^* = t + \tilde{t}$ where $\tilde{t}$ denotes preview time. Firstly, the measurement block can detect a desirable hand position $\boldsymbol{r}_d(t^*)$ on the surface of the target object at future time t^*. Then, the potential spaces detected by camera are created around the target object at the planning block automatically. Next, the planning block outputs desired joint angle $\tilde{\boldsymbol{q}}_d(t^*)$ corresponding to

Table 1 ${}^1S$ of $Peaki^*$ in global trajectory

$t[s]$	$Peak1^*$	$Peak2^*$	$Peak3^*$	$Peak4^*$
0	20140.69	14443.42	10762.14	14661.14
5	19650.81	14997.29	11305.17	14363.01
10	18684.81	14711.02	11350.10	13794.14
15	13067.19	12637.86	10914.79	< 0
20	13441.03	10656.65	11113.94	< 0
25	14803.23	11752.52	11539.66	< 0
30	13614.74	8505.96	7821.52	< 0
35	15327.24	11976.49	9622.34	< 0
40	16399.25	12404.49	13386.48	< 0
50	14656.65	11800.18	14204.03	< 0

future time t^* satisfying non-collision found by 1-Step GA. This is called by "imaginary manipulator". At last, the control block outputs desired joint angular velocity $\dot{\boldsymbol{q}}_d(t)$ that can control current joint angle $\boldsymbol{q}(t)$ to close the future desired joint angle $\tilde{\boldsymbol{q}}_d(t^*)$ to satisfy non-collision requirement.

When desired velocity $\dot{\boldsymbol{r}}_d(t)$ is given, the solution $\dot{\boldsymbol{q}}_d(t)$ is shown in (19) according to (2).

$$\dot{\boldsymbol{q}}_d(t) = \boldsymbol{J}^+(\boldsymbol{q})\dot{\boldsymbol{r}}_d(t) + (\boldsymbol{I}_n - \boldsymbol{J}^+(\boldsymbol{q})\boldsymbol{J}(\boldsymbol{q}))\boldsymbol{v}(t) \quad (19)$$

where, $\boldsymbol{J}^+(\boldsymbol{q})$ is pseudo-inverse of Jacobian matrix $\boldsymbol{J}(\boldsymbol{q})$, and $\boldsymbol{I}_n$ is $n \times n$ unit matrix. In Addition, $\boldsymbol{v}(t)$ is an arbitrary vector, trajectory tracking and obstacle avoidance can be executed simultaneously through this vector. Here, control variable $\boldsymbol{v}(t)$ is determined so as to make current joint angle $\boldsymbol{q}(t)$ of actual manipulator close to future joint angle of imaginary manipulator $\tilde{\boldsymbol{q}}_d(t^*)$ to satisfy non-collision requirement, so it is defined by (20).

$$\boldsymbol{v}(t) = \boldsymbol{K}_v[\tilde{\boldsymbol{q}}_d(t^*) - \boldsymbol{q}(t)] \quad (20)$$

where, $\boldsymbol{K}_v$ is a positive definite diagonal matrix representing gains, that is, $\boldsymbol{K}_v = diag[k_{v1}, k_{v2}, \cdots, k_{vn}]$.

Substituting (20) into (19) constitutes preview control system which use the future optimal joint angle $\tilde{\boldsymbol{q}}_d(t^*)$ satisfying non-collision requirement to control current configuration $\boldsymbol{q}(t)$. In reality, (20) is single-preview control because it just uses one future optimal configuration of imaginary manipulator at future time $t^* = t + \tilde{t}$ to control current configuration of actual manipulator at current time t to make current configuration close the future optimal configuration without collision. When we adopt single-preview control to control current configuration of actual manipulator, maximun ${}^1S$ found by 1-step GA ${}^1S_{GAmax}$ and the configuration corresponding to ${}^1S_{GAmax}$ when $t^* = 11[s]$ are shown Fig.10. ${}^1S_{GAmax}$ and the configuration corresponding to it when $t^* = 12[s]$ are shown in Fig.11. According to Fig.10 and Fig.11, we can find the optimal configuration when $t^* = 11[s]$ shown in Fig.10(b) can not reach the optimal configuration when $t^* = 12[s]$ shown in Fig.11(b) because there is a dangerous area described by black color between them found by comparing Fig.10(a) with

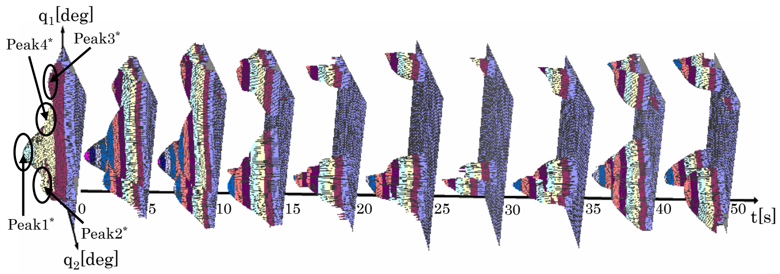

Fig. 8 3-D AMSIP ^1S distribution in whole tracking process

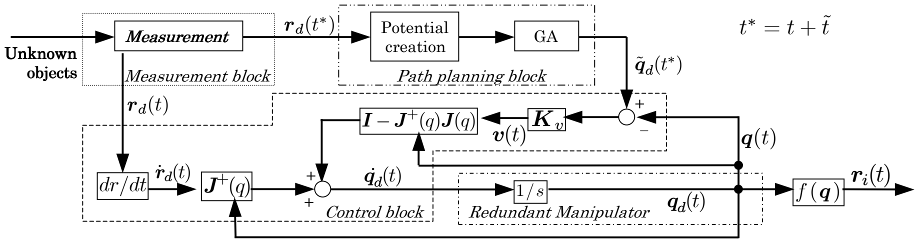

Fig. 9 Preview control system

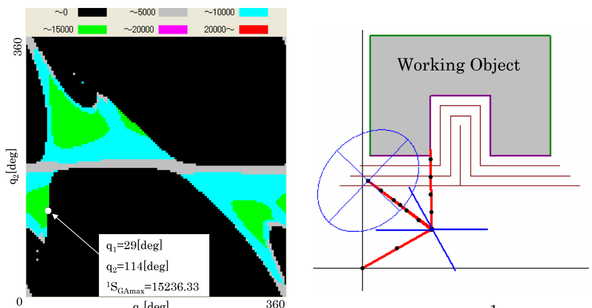

(a) $^1S_{GAmax}$

(b) Configuration of $^1S_{GAmax}$

Fig. 10 $^1S_{GAmax}$ and configuration corresponding to $^1S_{GAmax}$ found by 1-step GA when $t^* = 11[s]$

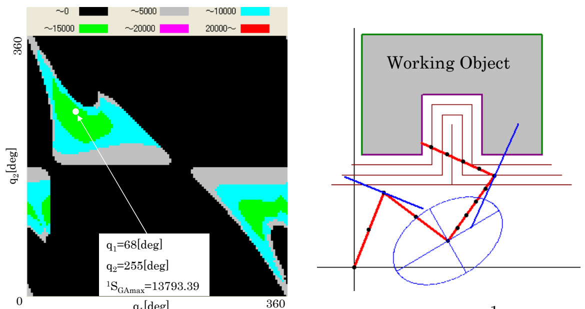

(a) $^1S_{GAmax}$

(b) Configuration of $^1S_{GAmax}$

Fig. 11 $^1S_{GAmax}$ and configuration corresponding to $^1S_{GAmax}$ found by 1-step GA when $t^* = 12[s]$

Fig.11(a) (here, note that Fig.10(a) and Fig.11(a) are 2-D distribution of ^1S, both coordinate axes denote the joint angles of link1 q_1 and link2 q_2 respectively whose ranges both are $[0°, 360°]$, the different pair of q_1 and q_2 corresponds to the different distribution range of ^1S described by six kinds of color area, i.e., black area corresponds to the distribution that $^1S < 0$, which indicates either collision has been occurred or manipulator's hand can not reach the goal position). In this condition, it is obvious that just using one future optimal configuration can not solve reachability of current configuration becuse information of changing environments is very limited. In this time, limitation of Local Method is embodied completely.

5.3 Multi-Preview Control

Multi-preview control is described as using several optimal configurations at future times $t_i{}^* = t + i\tilde{t}$, $(i = 1, 2, 3, \cdots, p)$ to control current configuration at current time t to make current configuration not only close the future optimal configuration without collision but also keep high reachability. Notice that p denotes the number of preview control we adopt, in other words, p denotes the number of imaginary manipulator. i.e., $p = 3$, it means that we adopt three future optimal configurations at three different future times $t + \tilde{t}$, $t + 2\tilde{t}$ and $t + 3\tilde{t}$ to control current configuration. In this way, control variable $\boldsymbol{v}(t)$ in (19) can be defined by (21).

$$\boldsymbol{v}(t) = \boldsymbol{K}_v[\sum_{i=1}^{p} k_i \tilde{\boldsymbol{q}}_d(t_i{}^*) - \boldsymbol{q}(t)] \tag{21}$$

where, $\boldsymbol{K}_v$ is a positive definite diagonal matrix representing gains as $\boldsymbol{K}_v = diag[k_{v1}, k_{v2}, \cdots, k_{vn}]$. $\sum_{i=1}^{p} k_i \tilde{\boldsymbol{q}}_d(t_i{}^*)$ is future optimal configuration obtained by using multi-preview control (it is obtained by considering several future optimal configurations), k_i are weight coefficients satisfying $0 < k_i < 1$ and $\sum_{i=1}^{p} k_i = 1$. We can select arbitrary value of preview time $\tilde{t}$ and number of preview control p and weight coefficient k_i according to different requirement. In a word, it is obvious that using multi-preview control can obtain more information of changing environments, which can improve the limitation of Local Method effectively.

6. ON-LINE OPTIMIZATION OF AMSIP USING 1-STEP GENETIC ALGORITHM

Among the many solutions, 1-step GA is used to search the optimal angles $\tilde{\boldsymbol{q}}_d(t^*)$ at future times $t_i{}^*$ to realize real-time optimization. In this research, the process of using camera to discern the instantaneous trajec-

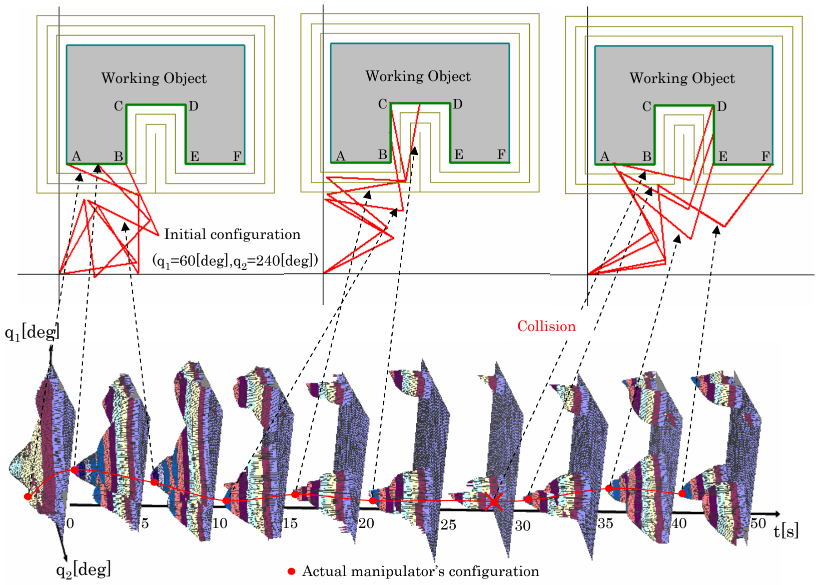

Fig. 12 Actual manipulator's configurations in whole tracking process when we use single-preview control

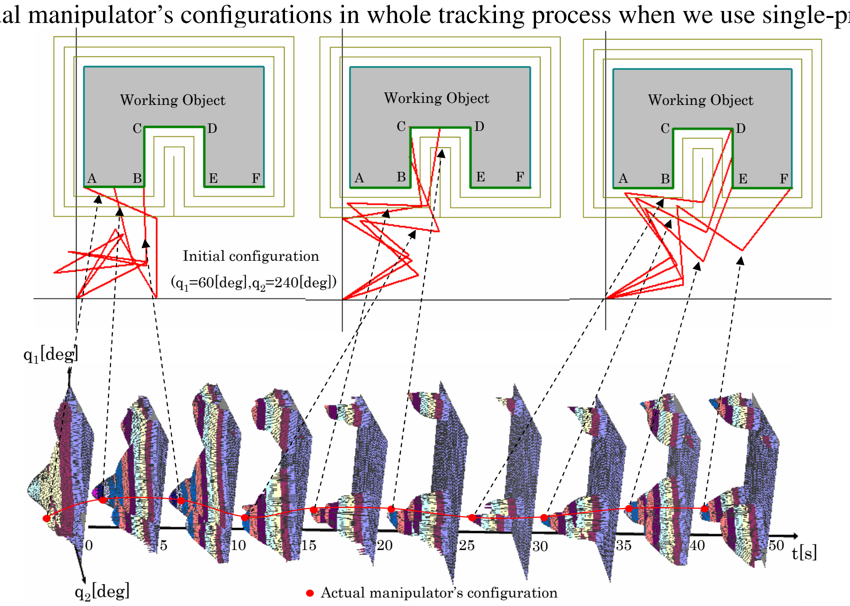

Fig. 13 Actual manipulator's configurations in whole tracking process when we use three-preview control

Table 2 The results found by 1-step GA

Position	$q_{GA1}[deg]$	$q_{GA2}[deg]$	${}^1S_{GAmax}$
A	82	105	20140.69
B	51	102	18684.81
C	24	101	12576.11
D	34	102	12537.59
E	26	98	16370.84
F	8	84	14656.65

Table 3 The results found by global exploration

Position	$q_{Max1}[deg]$	$q_{Max2}[deg]$	${}^1S_{Max}$
A	82	105	20140.69
B	51	102	18684.81
C	30	100	13441.03
D	30	100	13614.74
E	25	97	16399.25
F	8	84	14656.65

tory will be finished in 33 milliseconds. However, simulation shows that the maximun AMSIP value can be obtained using common GA method through about 30 generations and this process will cost 61 milliseconds or so. In this way, when the optimal configuration of manipulator using common GA method is obtained, the trajectory will move to other position and manipulator will not finish desired tracking. According to above discussion, it is required that better individuals must be found out as quickly as possible within 33 milliseconds. Therefore, in this paper, 1-step GA is adopted. By using 1-step GA, the results of experiment searching the optimal configurations when the manipulator's hand is fixed at six given positions are generalized in Table 2, where ${}^1S_{GAmax}$ denotes the optimal ${}^1S$ found by 1-step GA and q_{GA1} and q_{GA2} denote the joint angles of link1 and link2 corresponding to ${}^1S_{GAmax}$. In addition, we use global exploration method to do same experiment, the results are generalized in Table 3, where ${}^1S_{Max}$ denotes the real optimal

^{1}S in global zone and q_{Max1} and q_{Max2} denote the joint angles of link1 and link2 corresponding to $^{1}S_{Max}$. By comparing Table 2 with Table 3, it is clear that $^{1}S_{GAmax}$ is very near real optimal $^{1}S_{Max}$, which shows 1-step GA is very effective.

7. SIMULATION

The trajectory consists of five parts, shown as $A-B$, $B-C$, $C-D$, $D-E$ and $E-F$ respectively. The coordinate of A is fixed at position of $(10cm, 140cm)$, the each length of trajectory is defined as $l_{A-B} = l_{B-C} = l_{C-D} = l_{D-E} = l_{E-F} = 75[cm]$ and the length of each link is defined as $l_1 = l_2 = l_3 = l_4 = 75[cm]$. The whole simulation time is set by 50 seconds.

7.1 Simulation of Single-Preview Control

Firstly, we use single-preview control to do some simulations and the single-preview time $\tilde{t}$ is set by 10 seconds. ^{1}S of actual manipulator at ten different given times in whole tracking process denoted by red points and configurations corresponding to ^{1}S at these ten times are shown in Fig.12, where the red line connecting these red points denotes the trajectory changings of ^{1}S of actural manipulator in whole tracking process. From Fig.12, we can find that actual manipulator almost can achieve on-line trajectory tracking except for the collision with working object when $t = 30[s]$.

7.2 Simulation of Multi-Preview Control

Here, we adopt three-preview control to do the same simulations, three future times are defined by $t_1{}^* = t+\tilde{t}$, $t_2{}^* = t+2\tilde{t}$ and $t_3{}^* = t+3\tilde{t}$ respectively (here, $\tilde{t} = 5[s]$). Then, we define $k_1 = 0.3$, $k_2 = 0.65$ and $k_3 = 0.05$ (notice that weight coefficients k_i has been presented in (21). In this way, we use three future optimal configurations of imaginary manipulators at $t_1{}^*$ $(t+5[s])$, $t_2{}^*$ $(t+10[s])$ and $t_3{}^*$ $(t+15[s])$ (use more information of future changing environments) to control current configuration of actual manipulator. The simulation result is shown in Fig.13. From Fig.13, we can find that collision occurred at $30[s]$ by using single-preview control has been avoided by using three-preview control and actual manipulator can achieve on-line trajectory tracking without collision meanwhile keeping higher avoidance manipulability.

8. CONCLUSION

This paper proposes a new approach using multi-preview control system to solve a on-line trajectory tracking and obstacle avoidance problem for redundant manipulator based on considering reachability. By simulations, we verify the validity of multi-preview control through simulations of comparing single-preview control with multi-preview control. Therefore, we think that multi-preview control method can improve limitation of Local Method in a large extent.

REFERENCES

[1] Rodrigo S. Jamisola, Jr. Anthony A. Maciejewski, Rodney G. Roberts “Failure-Tolerant Path Planning for Kinematically Redundant Manipulators Anticipating Locked-Joint Failures”, IEEE Transactions on Robotics, Vol.22, No.4, pp.603-612, 2006.

[2] Juan Manuel Ahuactzin, Kamal K. Gupta “The Kinematic Roadmap: A Motion Planning Based Global Approach for Inverse Kinematics of Redundant Robots”, IEEE Transactions on Robotics and Automation, Vol.15,No.4,pp.653-669, 1999.

[3] Leon Zlajpah, Bojan Nemec “Kinematic Control Algorithms for On-line Obstacle Avoidance for Redundant Manipulator”, International Conference on Intelligent Robots and Systems, pp.1898-1903, 2002.

[4] Homayoun Seraji, Bruce Bon “Real-Time Collsion Avoidance for Position-Controlled Manipulators”, IEEE Transactions on Robotics and Automation, Vol.15, No.4, pp.670-677, 1999.

[5] Mamoru Minami, Yoshihiro Nomura, Toshiyuki Asakura “Avoidance Manipulability of Redundant Manipulators ”, Journal of the Robotics Society of Japan, Vol.17, No.6, pp.887-895, 1999.

[6] M. Minami, J. Agubanhan, T. Asakura “Manipulator Visual Servoing and Tracking of Fish using Genetic Algorithm”, Int. J. of Industrial Robot, Vol.29, No.4, pp.278-289, 1999.

[7] M. Minami, J. Agubanhan, T. Asakura “Robust Scene Recognition using a GA and Real-world Raw-image”, Measurement, Vol.29, pp.249-267, 2001.

[8] Keiji Ikeda, Hiroshi Tanaka, Tong-xiao Zhang, Mamoru Minami, Yasushi Mae “On-line Optimization of Avoidance Ability for Redundant Manipulator”, International Conference on Intelligent Robots and Systems, pp.592-597, 2006.

[9] Mamoru MINAMI, Yoshihiro NOMURA, Tosiyuki ASAKURA “Trajectry Tracking and Obstacle Avoidance Control to Unknown Objects for Redundant Manipulators Utilizing Preview Control”, Transactions of the Japan Society of Mechanical Engineers, no.95-1813, pp.3543-3550, 1996.

[10] Mamoru MINAMI, Yoshihiro NOMURA, Tosiyuki ASAKURA “Preview and Postview Control System for Tajectry Tracking and Obstacle Avoidance to Unknown Objects for Redundant Manipulators”, Transactions of the Japan Society of Mechanical Engineers, vol.15, no.4, pp.573-580, 1997.